

# F61: Nuclear magnetic resonance spectroscopy

THIMO PREIS AND TOBIAS ABELE\*

Karl-Ruprechts-Universität Heidelberg

26.03-30.03.2018

## Abstract

*The goal of this experiment is to test methods of nuclear magnetic resonance with two different NMR analyzers. In detail we want to determine the spin-spin and spin-lattice relaxation time for two samples with different concentrations of Gadolinium solved in water with the usage of the Bruker minispec p20 apparatus. Measurement of the former quantity is carried out via the spin echo as well as the Carr-Purcell method. With the same setup we furthermore measured the chemical shift of protons and used it to identify five different substances. The Bruker minispec mq7.5 is used for imaging measurements in one and two dimensions. One dimensional processes such as the time dependent mixture of oil and sand are analyzed and two dimensional imaging is used to map the inner volume of samples which contain oil or water.*

## I. THEORY

### 1. Relaxation time

A macroscopic probe consists of many atoms, each of which with a nucleus carrying a spin and thus a magnetic dipole moment  $\mu_I = \hbar\gamma_I\vec{I}$ . The spins try to align either parallelly or antiparallelly to an applied external magnetic field  $B_0$ . Restricting the discussion to protons we expect an effective magnetization in direction of  $\vec{B}_0$  due to them having the tendency to occupy the energetically more favorable state, according to the Fermi-Dirac statistic. Disrupting the macroscopic magnetization from equilibrium will always lead to the same macroscopic magnetization after some time, because the systems wants to minimize its total energy according to the principle of least action. This Process is called relaxation and we distinguish between two different kinds of relaxation.[1]

---

\*Under the supervision of Minjung Kim

### 1.1 Spin-Spin relaxation $T_2$

The spin-spin relaxation is caused by the interaction between distinct spins amongst themselves. The transverse magnetization gets decreased via the dephasing of the coherent movement of the spin magnetic moments. The characteristic relaxation time of this process is called spin-spin relaxation time  $T_2$ . The Bloch equations describe the time evolution of the magnetization subject to relaxation. From them one can derive the time evolution of the transverse magnetization to be determined by the spin-spin relaxation time via [1]

$$M_{\perp}(t) = M_{\perp}^0 e^{-\frac{t}{T_2}} \quad (1)$$

### 1.2 Spin-Lattice relaxation time $T_1$

The spin-lattice relaxation time describes the interaction between the spins with the external magnetic field. The energy emitted by a system out of equilibrium dissipating to its equilibrium state, thus attaining an effective equilibrium magnetization, is absorbed by the lattice. The characteristic time scale of this relaxation process caused in this interaction is called spin-lattice relaxation time  $T_1$ . The time evolution of the magnetization component (anti-)parallel to the external magnetic field  $B_0$  is again determined by the Bloch equations via the spin-lattice relaxation time to be [1] [3]

$$M_{\parallel}(t) = M_{\parallel}^0 \left(1 - 2e^{-\frac{t}{T_1}}\right) \quad (2)$$

## 2. Chemical shift

Chemical shift is, besides dipole-dipole interaction and internal coupling, one of the main internal interactions of magnetic dipole moments. It accounts for an additional magnetic field caused by the electrons surrounding the magnetic dipole moments of the nucleus. The proportionality factor between the additional and the external magnetic field is molecule specific and is called magnetic shielding factor (measured in parts per million). The Hamiltonian of the observed system is given by

$$H = H_Z + H_C + H_J + H_D \quad (3)$$

where  $H_Z$  represents the Zeeman splitting caused by the external magnetic field  $B_0$  and  $H_D$  accounts for the dipole-dipole interaction (is averaged out in fluids). The electrons weaken the magnetic field around the nucleus proportionally to the external magnetic field, following Lenz's law, which in turn results in the chemical shift  $H_C = \hbar\gamma\sigma\vec{I}\vec{B}_0$ . The additional term  $H_J = J_{12}\vec{I}_1\vec{I}_2$  is caused by the indirect coupling between two magnetic dipole moments in a molecule via the electrons,  $J_{12}$  describes the coupling factor. The Brownian motion is responsible for averaging out the splitting of the spectrum caused by the indirect coupling in different molecules.[2] [5]

### 3. Imaging with NMR

A static, spatially homogeneous magnetic field is not sufficient for image taking, because all spins would have the same larmor frequency. One excitation pulse would therefore always excite the entire sample. We can spatially localize the amount of hydrogen atoms at one point by applying a gradient field, because the larmor frequency is proportional to the magnetic field and which in turn is proportional to the spatial position. We can split the sample into slices in e.g. the xy-plane by applying a magnetic gradient in z-direction, because this results in the precession motion of every slice to have a different larmor frequency:

$$\omega_{Larmor} = \gamma (B_0 + B^z(z)) \quad (4)$$

One can therefore guarantee spins of a specific slice to go in resonance with the frequency applied to the rotating magnetic field and then measure the relaxation time, this is called frequency coding. The stronger the applied magnetic gradient the thinner a given slice in the xy-plane becomes.

We can furthermore apply a phase encoding gradient to dephase spins along the vertical axis (y-axis). The gradient is only applied for a short amount of time such that, after the gradient has been shut down, we observe different phases between the spins along the y-axis, hence we now can decode the y-position via the phase with a spin echo measurement (compare 1.1), this is called phase coding. The resolution of this localization is limited by the measurement only being able to distinguish two phases with a difference less than  $2\pi$ .

We can finally apply a third gradient field in x-direction during the echo, this results in the z-gradient field to increase along the x-direction such that the larmor frequencies along the x-axis increase with an increase in magnetic field strength. The measured echo of the magnetic resonance signal now consists of a broad frequency spectrum, but now we can identify the spatial point via the specific larmor frequency. One can now use either frequency or phase coding in order to acquire a 1D image of the sample via a one dimensional Fourier transformation of the measured NMR signal, where now every point in position space corresponds either to a specific frequency or a specific phase.

One can also use both methods in order to make a two dimensional image measurement. One first selects a slice by an appropriate combination of gradient field and high frequency pulse. Within the slice, two dimensional position information is derived by a combination of phase coding in x-direction and frequency coding in y-direction. One now proceeds to make  $N$  measurements, each consisting of a combination of frequency and phase coding, with different values of the phase coding gradients in x-direction. During every measurement the NMR signal is read out at different times  $t_m$  with  $m \in \{1, M\}$ . The two dimensional matrix of the image is then finally derived via a two dimensional Fourier transformation of the matrix consisting of  $N \times M$  data points.[1]

## II. EXPERIMENTAL SETUP AND MEASUREMENT PRINCIPLES

### 1. Measurement of relaxation times and chemical shift

In the first part of the experiment the spin-lattice relaxation time  $T_1$  and the spin-spin relaxation time  $T_2$  are measured. The spin-spin relaxation time is measured by the spin echo (compare 1.1) as well as by the Carr-Purcell method (compare 1.2). The chemical shift of protons is measured in the following and used to identify five different substances. These measurements are carried out with a Bruker minispec p20, it consists of a Minispec p20 Electronic Unit used signal generation and of a Minispec p20 magnet with a static magnetic field  $B_0$ . The magnet is shielded by a styrofoam material for minimal temperature variation when in use. One can now generate a magnetization  $M_\perp$  perpendicular or  $M_\parallel$  antiparallel to  $\vec{B}$  by applying a high frequency pulse  $\omega_{HF}$  via the electronic unit to the ground state magnetization  $\vec{M}$ . We can now rotate the macroscopic magnetization by an angle  $\alpha = \gamma_I B_1 \Delta t$  by applying a sinusoidal voltage of given frequency  $\omega_{HF}$  for a given time duration  $\Delta t$  to a coil oriented perpendicular to the static magnetic field  $B_0$ . This result in a solenoidal magnetic field  $\vec{B}_1$  which is longitudinally polarized parallel to the orientation of the coil. The rotated macroscopic magnetization now precesses around the  $B_0$  magnetic field. This in turn induces a voltage into the same coil, which then again represents our measurement signal, which is a mixed signal partially consisting of the so-called working frequency. It is the difference  $\nu_{work} = \omega_{HF} - \omega_{Larmor}$  and it has to be calibrated to a value of around  $1kHz$  by varying the larmor frequency via varying the static magnetic field.. One can furthermore vary the time duration of the applied voltage in order to rotate the magnetization by an angle  $\alpha = 90^\circ, 180^\circ$  into its perpendicular or antiparallel component with respect to the orientation of  $\vec{B}_0$ . [1]

#### 1.1 Spin echo

In order to measure the spin-spin relaxation time  $T_2$  according to 1 one starts with a  $90^\circ$  pulse in order to create a transverse magnetization in y-direction, such that it will precess around the static magnetic field  $B_0$  with a given larmor frequency  $\omega_{Larmor} = \gamma B_0$ .

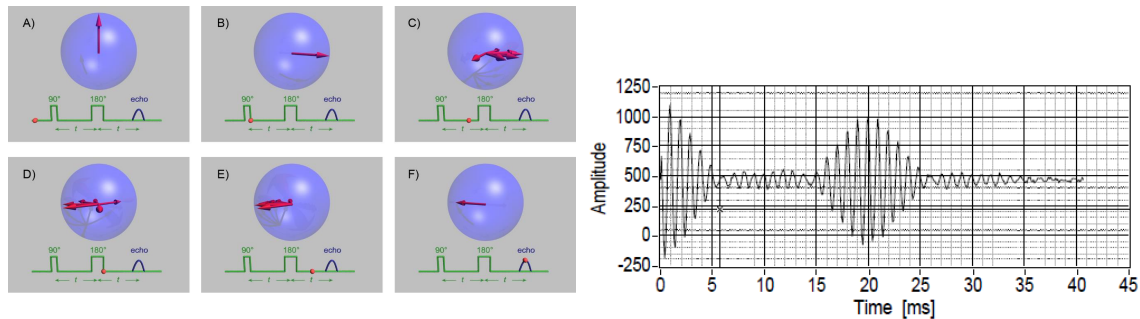


**Figure 1:** From left to right: Spin echo method [6], output signal [1]

Protons at different positions in the probe will now precess with different Larmor frequencies due to the inhomogeneity of the field, thus phase difference between the protons will develop. One can now revert the phases of the spins with a  $180^\circ$  pulse in order to guarantee all protons of given phases to coherently align after a given time interval of two times the so-called spin-echo time  $\tau$ . The induced signal then again represents the relaxation time for the transverse magnetization, which is dominantly caused by spin-spin interactions, thus  $T_2$ . [1]

## 1.2 Carr-Purcell sequence

One only achieves approximate alignment of the magnetic dipole moments after  $2\tau$  for long spin echo times due to molecular diffusion happening before the  $180^\circ$  pulse can be applied. The Carr-Purcell sequence minimizes the effects of molecular diffusion and field inhomogeneities by starting the sequence with a  $90^\circ$  pulse followed up by a  $180^\circ$  pulse to ensure phase coherence of the system after  $t = 2\tau$ . One now applies further  $180^\circ$  pulses for every odd multiple of  $\tau$  in order to guarantee phase coherence for every even multiple of  $\tau$ . A measurement of the spin-spin relaxation time by the Carr-Purcell

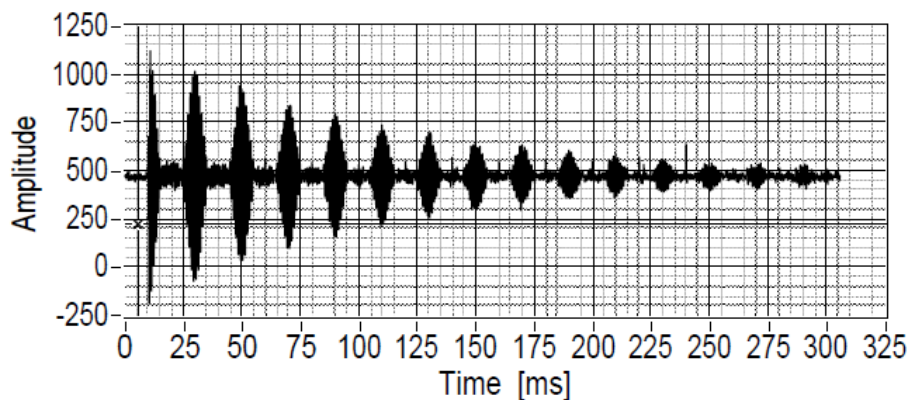
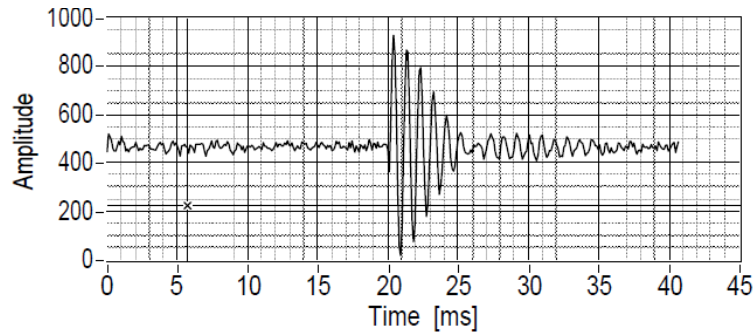


Figure 2: Carr-Purcell sequence [1]

method hence yields a value which is closer to the true value of the system as compared to the measurement with the spin echo method.[1]

## 1.3 Measurement of spin-lattice relaxation $T_1$

One produces a magnetization antiparallel to the static magnetic field by starting the measurement with the generation of a  $180^\circ$  pulse. By following this up with a  $90^\circ$  pulse one measures a signal which represents the current longitudinal magnetization, which is due to spin-lattice interactions and can therefore be used to measure  $T_1$ . [1]



**Figure 3:** Pulse sequence  $180^\circ$ - $90^\circ$  with  $\tau = 20\text{ms}$  [1]

## 2. Imaging with NMR - Das hier könnte man ganz streichen

The imaging measurements are made with the Bruker NMR analyzer mq7.5, where the gradient fields were applied via a system of Helmholtz coils. Nuclear Magnetic Resonance techniques are used for imaging measurements in one and two dimensions. The flow of oil in sand is measured as a time dependent process in one dimension. Two dimensional measurements are carried out to map the inner volume of substances which contain oil or water. The measurement principle of this apparatus is described within 3.[1]

## III. DATA ANALYSIS

### 1. Measurement of relaxation times

Both the spin-spin and the spin-lattice relaxation time have been measured with the use of two different concentrations of Gadolinium solved in water, one solution with 500 water molecules per Gadolinium atom (Gd500) and the other solution containing 600 water molecules per Gadolinium atom (Gd600). The measured values were acquired by a fit of their respective fit functions 1 for  $T_2$  and 2 for  $T_1$  applied to the measured data 4

	Gd500	Gd600
$T_2$	$(99.8 \pm 0.5_{stat}) \text{ ms}$	$(129 \pm 1_{stat}) \text{ ms}$
$T_2(\text{CP})$	$(124.0 \pm 0.4_{stat}) \text{ ms}$	$(150.6 \pm 0.6_{stat}) \text{ ms}$
$T_1$	$(118.8 \pm 2.2_{stat}) \text{ ms}$	$(135.8 \pm 1.2_{stat}) \text{ ms}$

**Table 1:** Measured Values

Pulse I has to be maximized in order to represent a  $90^\circ$  pulse, it was set to  $\approx 2.1$ , and Pulse II has to be minimized in order to be a  $180^\circ$ , it was set to  $\approx 2.2$ . We acquired a data point at 900ms echo time for the  $T_1$  Gd500 measurement which we decided to exclude from the fitted dataset as it was way higher than one would theoretically expect.

We found the reason for this to be the sensitivity of the measurement configuration to the background noise, because we changed the integrated over peak window before the aquirement of said data point. One theoretically expects  $T_2(\text{CP})$  to be larger than  $T_1$  for both solutions, because the spin-spin interaction dominates  $T_2$ : Dipoles want to align in the energetically most favourable way, antiparallel. This alignment proceeds faster in comparison to the spin-lattice interaction important for the  $T_1$  measurement.  $T_1$  describes the average time needed for the mean magnetization to go over from antiparallel to parallel alignment with respect to the external magnetic field, this is microscopically described by single spins orienting themselves from  $-1/2$  to  $+1/2$ . [1] We observe our expectation of  $T_2$  (CP) being larger and more precise than  $T_2$ , as explained in 1.2, to be true.

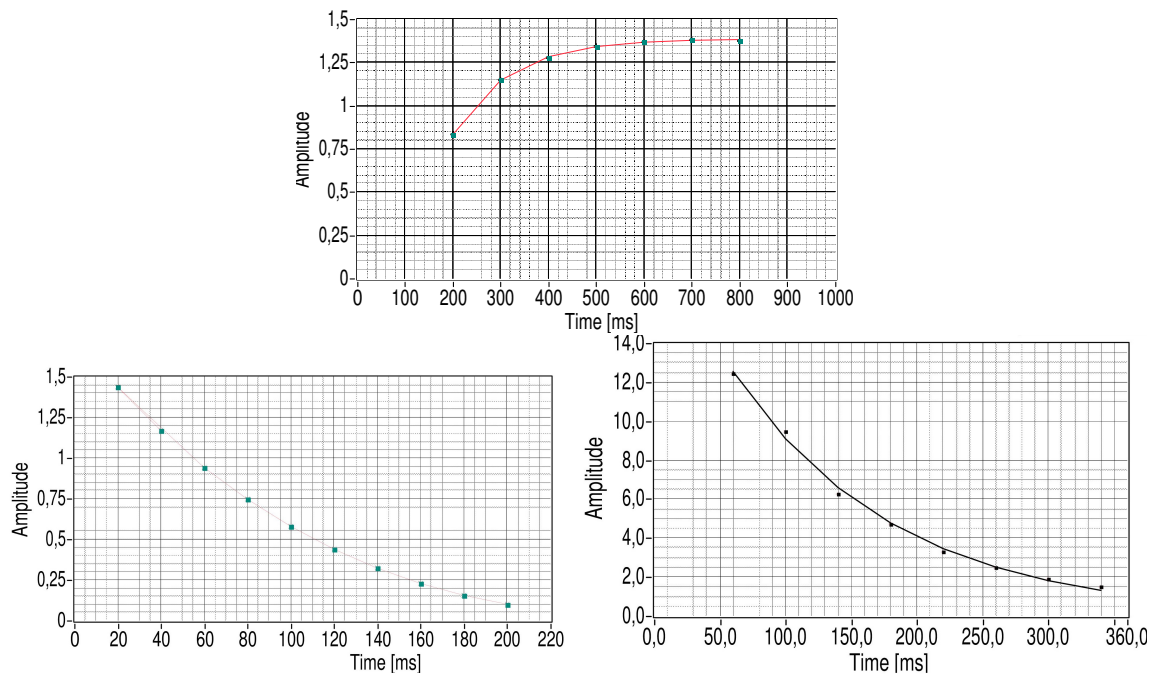


**Figure 4:** In the top row: spin-lattice relaxation time  $T_1$  in Gd500 with spin-echo method  
 From left to right in the bottom row: spin-spin relaxation time  $T_2$  in Gd500 with spin-echo method and spin-spin relaxation time  $T_2$  in Gd500 with the Carr-Purcell (CP) method

We furthermore observe the relaxation times of Gd500 to be shorter than for Gd600. Gadolinium is strongly paramagnetic and is magnetized at room temperature (Curie point at  $\approx 19^\circ\text{C}$ ). The form of paramagnetism exhibited by Gadolinium compounds derives from electrons, not protons, and is known as Curie paramagnetism. Because of electrons having  $s = 1/2$ , but a much smaller size than the proton, their gyromagnetic ratio is  $\approx 657$  times larger. If the electrons remain unpaired in shells or bonding orbitals, the unbalanced spin produce a strong magnetic moment capable of inducing magnetic relaxation in nearby nuclei. The seven unpaired electrons in the  $4f \rightarrow s_e = 7/2$  subshell therefore account for the elements strong paramagnetism. [4] The presence of such large

fluctuating paramagnetic moments in a solution thus has strong effects on the nuclear spin relaxation of the solvent water nuclei. Therefore, the more Gadolinium atoms available the more dipole-dipole interactions between the water molecules and the Gadolinium atoms are possible and the shorter is the relaxation time. Instead we measured exactly the opposite to be true 1. We therefore repeated our measurement for  $T_2(\text{CP})$  and for  $T_1$  with the Gd600 probe and a more narrow peak window to further exclude background noise.  $T_2(\text{Cp})$  didn't change much, but the new value for  $T_1$  was  $T_1 = (251.9 \pm 4.7_{\text{stat}})$  ms and therefore met our theoretical expectations. Thus, again the use of the same configuration with a slightly more narrow peak window leads to a huge difference in measured values. The whole setup is therefore very sensitive to the integrated over peak window, which hence should be checked quite thoroughly in order to guarantee reproducibility of results in this section.

## 2. Chemical shift

In order to identify the different samples A-E with the given chemical substances (Toluene, P-Xylene, Acetic acid, Fluoroacetone, Fluoroacetonitril) we applied a  $90^\circ$  pulse on the respective samples and acquired via Fourier transformation a frequency spectrum as output signal in which the different Larmor frequencies were observable.

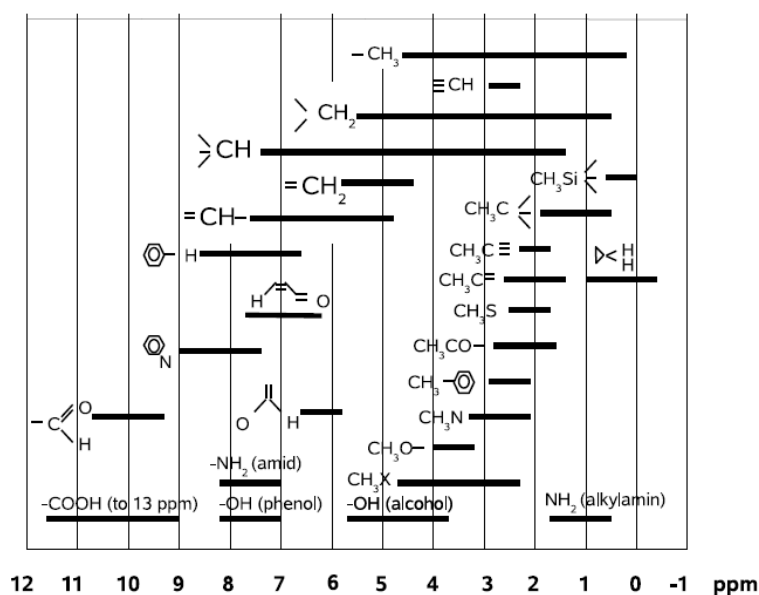


Figure 5: Chemical shift of compounds relative to TMS [1].

The sample was put into a rotating motion via compressed air in order to average out inhomogeneities within the external magnetic field - the respective peaks got clearly more narrow and more distinct. Rotating the sample near the relaxation time though messes up the system such that we constantly calibrated the applied working frequency



after every measurement to be at the order of  $\nu_{work} = (506 \pm 20)\text{Hz}$ . This was also necessary, because the experimental setup is not isolated very well such that drifts in the magnetic field due to temperature variation are, despite the short measurement time, not preventable. We furthermore measured samples A+-E+ which additionally contained the substance Tetramethylsilane (TMS). The hydrogen resonance line of TMS is located near the edge of the shown spectrum due to its high chemical shift, we can thus use this line as a reference in order to distinguish between different samples. With the difference between the peaks of the respective samples and the reference peak we can identify every sample via 5. For sample A+ and D there were no corresponding samples with/without TMS available such that we identified the TMS reference peak via the samples B+, C+, E+. We found the ppm position of said peak by averaging said samples to be at  $TMS = (31.30 \pm 0.12_{stat})\text{ ppm}$ . This value can in the following be used as a reference value for the sample D, where no D+ sample was available, and for identifying the reference value for A+, where no sample A was available.

In the following analysis one has to be aware of CO and CN not producing any resonance peak due to their nuclei having spin zero.

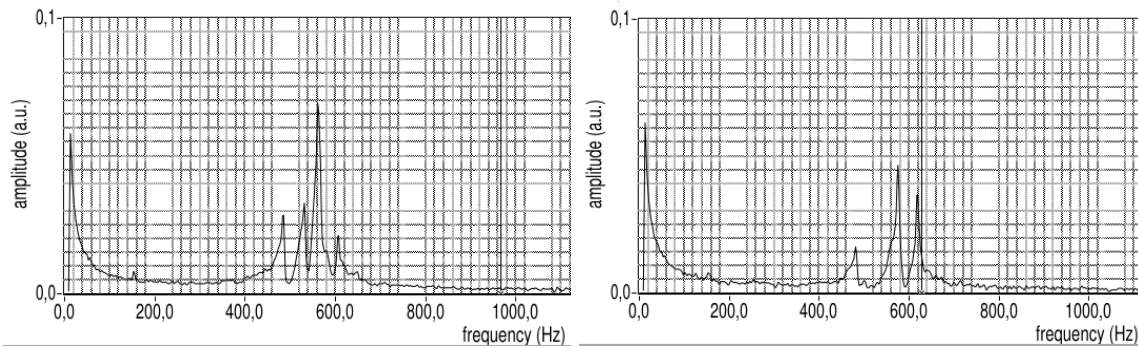


**Figure 6:** Frequency spectrum of the A+ (left) and of the B+ (right) sample

Peak	frequency [Hz]	ppm	difference to TMS	Substance
1	484.0	24.4	6.2	$FCH_2$
2	530.0	26.8	3.8	$FCH_2$
3	560.0	28.3	2.3	$CH_3$
4	606.0	30.6	Reference	

**Table 2:** Sample A+

Sample A is from 2 identified as Fluoroacetone. Fluorine atoms have an odd number of protons and an even number of neutrons in their nucleus such that they possess a nuclear spin of  $s = 1/2$ , this spin can couple parallelly or antiparallelly to the proton of the  $CH_2$  compound such that we can observe two peaks belonging to  $FCH_2$ . [7]

Sample B could either correspond to Toluene or to P-Xylene. By comparison with sample

Peak	frequency [Hz]	ppm	difference to TMS	Substance
1	480.0	24.2	6.9	Benzene
2	574.0	29.0	2.1	$CH_3$
3	616.0	31.1	Reference	

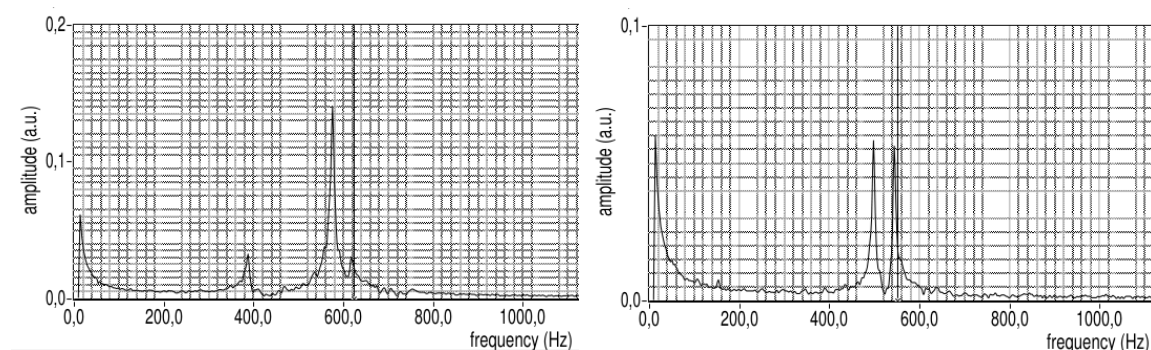
**Table 3:** Sample B+

E+ we find the intensity of peak 2 in 3 to be much larger than its corresponding value of sample E in 6 such that we identify sample B as p-Xylene.

Peak	frequency [Hz]	ppm	difference to TMS	Substance
1	386.0	19.5	11.6	COOH
2	573.9	29.0	2.1	$CH_3$
3	616.0	31.1	Reference	

**Table 4:** Sample C+

From this we identify sample C to be Acetic acid.

**Figure 7:** Frequency spectrum of the C+(left) and of the D (right) sample

Peak	frequency [Hz]	ppm	difference to TMS	Substance
1	496.0	25.1	6.2	$FCH_2$
2	542.1	27.4	3.9	$FCH_2$
3	$31.30 \pm 0.12$	31.1	Reference from E+, C+, B+	

**Table 5:** Sample D

As for sample A (compare 2) Fluorene couples either parallelly or antiparallely to the proton of the  $CH_2$  compound such that we observe two peaks of different frequency corresponding to the same molecule. We therefore identify sample D from 5 to be Fluoroacetonitril.

Peak	frequency [Hz]	ppm	difference to TMS	Substance
1	482.0	24.3	7.1	Benzene
2	580.0	29.3	2.1	$CH_3$
3	622.0	31.4	Reference	

**Table 6:** Sample E+

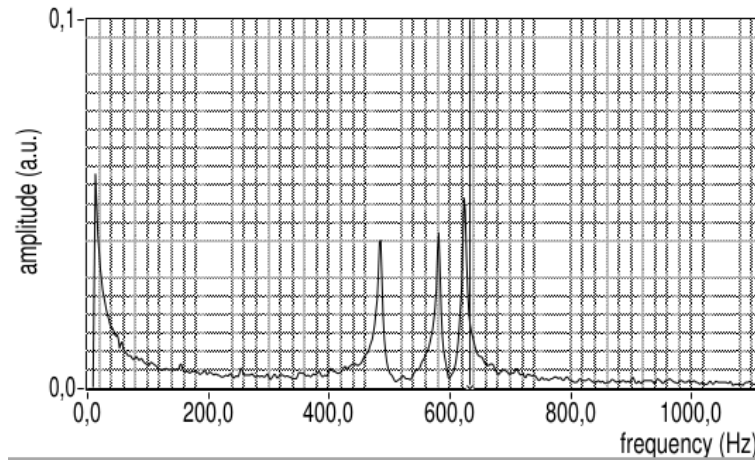


**Figure 8:** Frequency spectrum of the E+ sample

As discussed with sample B+ we identify sample E through comparison with 3 to be Toluene.

### 3. Imaging with NMR

#### 3.1 One dimensional imaging

The first two samples consisted of two glass tubes filled with 15mm and 50mm of oil respectively. The former sample produced a step function as output signal and the latter sample also produced a step function but with a broader width. We furthermore observe both samples to show different amplitudes in output signal due to inhomogeneities of the magnetic field and, furthermore, we observe both signals to be distorted by noise due to making a Fourier transformation of a finite dataset. The resulting images can be seen in figure 9.

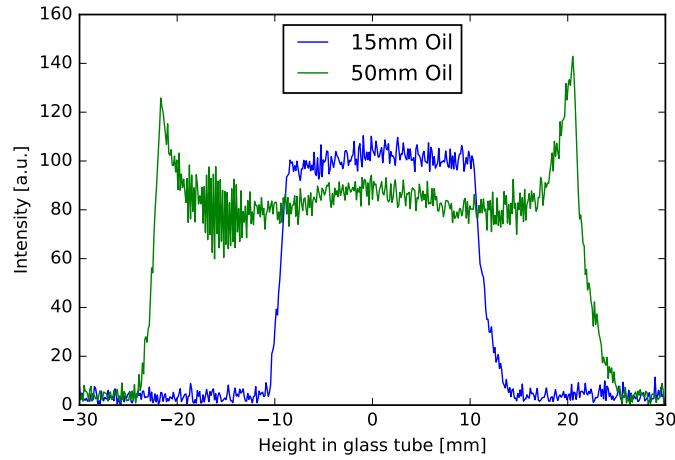


**Figure 9:** 1D imaging of 15 mm and 50 mm oil samples

The next sample contained a cylindrical piece of teflon in the form of seven concentric, similar, equidistant and parallel slices surrounded by oil. The acquired spectrographic

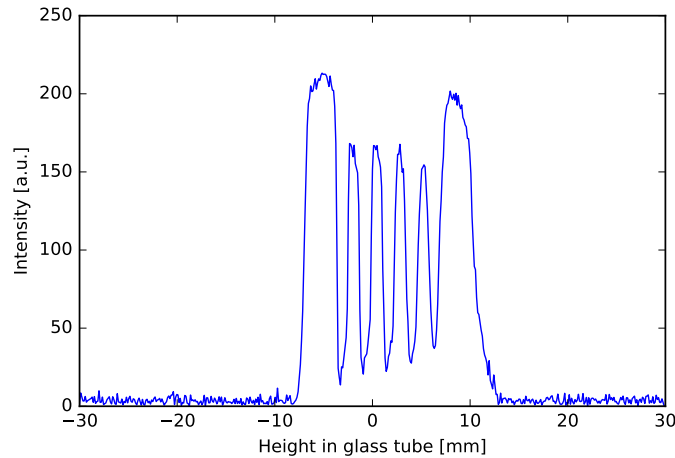


**Figure 10:** 1D imaging of an oil sample mixed with Teflon layers

image 10 shows diminished amplitudes in the center of the signal, because the seven slices are connected to a piece of plastic which holds said slices in place and which gives no signal. We can furthermore deduce from figure 10, that the thickness of the teflon layers ( $\approx 1.5\text{mm}$ ) is larger than the resolution of the Bruker NMR analyzer mq7.5 used in this setup, otherwise we would simply observe a step function for the whole sample due to the resolution not being high enough to show the oil layers in between the teflon slices. The resolution of the Bruker NMR analyzer mq7.5 was given by the manual to be  $< 1\text{mm}$ . It is limited by the least possible step size of the magnetic field in the measurement being

quite large, such that one cannot distinguish in small ranges of  $B$ , and by only performing a Fourier transformation of a finite set of datapoints, which in turn results only in an approximate representation of the input signal due to the Fourier transformation of the step function (hyperbolic sine) only having a finite number of main oscillations in the given dataset.

The fourth sample contained 15 mm of sand and approximately 4mm of oil on top. In the following we will answer the question whether this process of oil mixing with sand can be understood as a diffusion process. Figure 11 shows the measured data acquired in steps of 2 minutes in between every plotted line. The signal at first is simply a step-function with some background noise, which represents the input signal from the separated oil layer. The zero point on the x-axis therefore gives us the border between the oil and sand layer. The signal in the  $x < 0$  area gradually increases over time as the oil sinks more and more into the sand layer. The signal at the end of the mixing process should be a flat, noisy step function as it should represent one signal for the whole oil-sand mixture. We instead observe it not being completely flat, but having some small bumps in between. This is due to tightly bound sand granules in between the mixture which do not let the oil sink through to the bottom side of the glass tube, these areas therefore give no signal. The mixing of oil and sand observed here does not describe a diffusion process, because diffusion is described by a concave function [?]. We on the contrary measured this process to fall off like a convex function, as seen in 11.

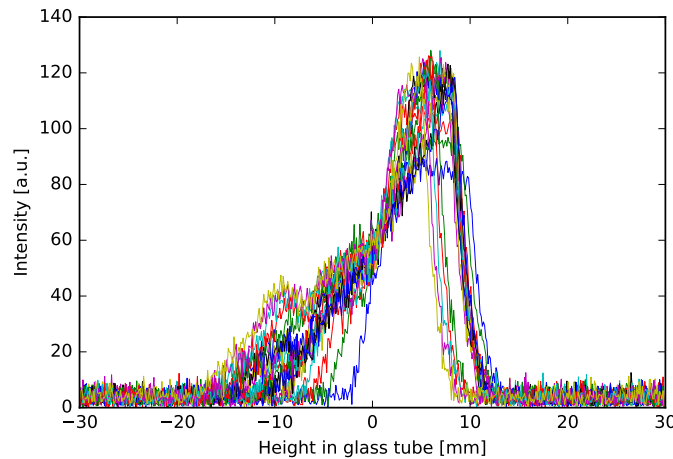


**Figure 11:** *Time dependent evolution of oil sinking into sand*

### 3.2 Two dimensional imaging

The first sample consisted of 15mm oil within a glass tube. For horizontal slicing we expected a circle, as the sample gives a signal at every point until the boundaries of the glass tube are met. The result can be seen in figure 12. The distortion of the circular image to the front is due to inhomogeneities of the magnetic field intrinsic to this machine, we

therefore concluded not to use back to front slicing in the following with this setup.

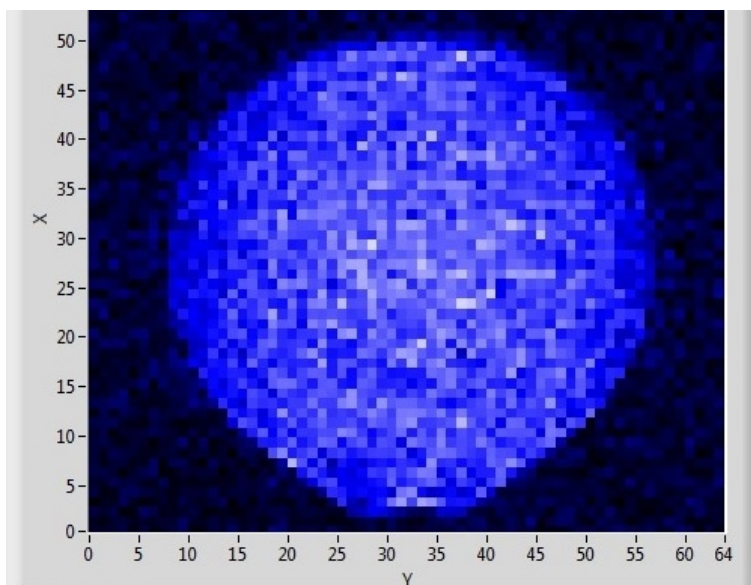


**Figure 12:** 15mm oil sample sliced back to front horizontally

We expect a square to show for left to right slicing, again due to the sample consistently giving a signal until the boundaries of the glass tube are met. The result of the left to right slicing can be seen in figure 13. The curve at the top of the slice is due to surface tension

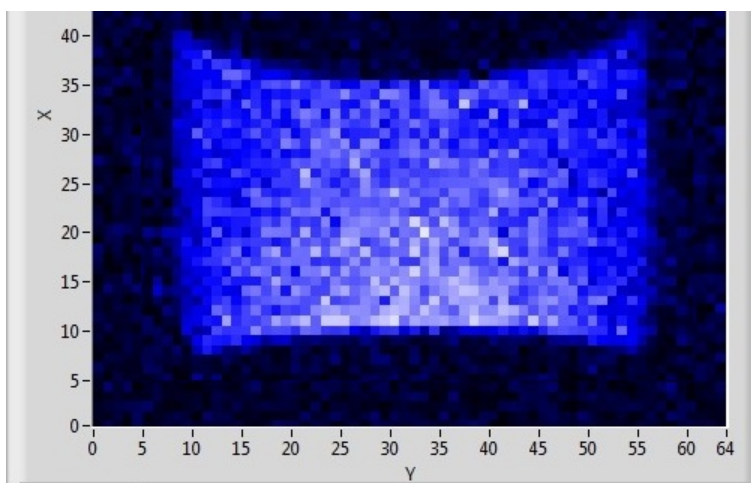


**Figure 13:** 15mm oil sample sliced vertically from left to right

between the oil and the glass tube. The flat edge at the bottom is due to the bottom side of the glass tube. Throughout the measurement we constantly checked the temperature in the Bruker NMR analyzer mq7.5, it stayed nearly constant and only changed by 0.001 °C.

We proceeded with taking twodimensional images of organic objects.

Figure 14 shows a peanut with shell. We can only observe one nut (the dark, elliptical object inside the upper cell), because the peanut wasn't completely centered in the glass tube such that the left to right slice only slices through one of the cells (the upper one with the nut shown) and only captures the beginning of the lower cell as the slice went right through the middle between the two cells.

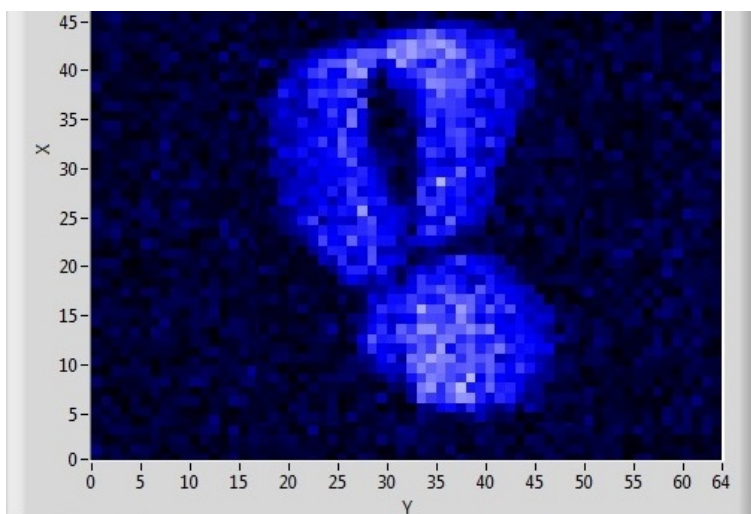


**Figure 14:** *Peanut inside shell sliced vertically from left to right*

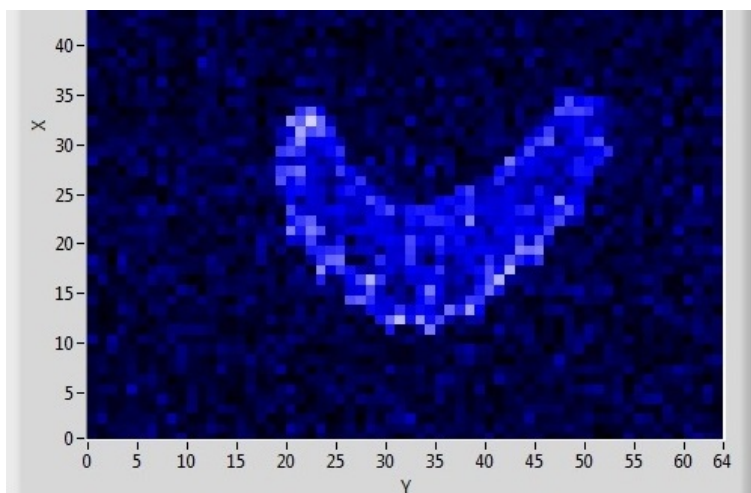


**Figure 15:** *Sample of celery sliced horizontally*

Figure 15 shows the C-shaped form of a piece of celery. This is the second image taken from the same sample as the first one only showed unidentifiable structure, because here no perfect gradient could be calibrated due to the sample not being placed perfectly inside the measurement boundaries of the Bruker NMR analyzer mq7.5.



Figure 16 in contrast shows an apple core sliced horizontally. The star shaped core contains apple seeds which do not give any signal, hence the black areas. The signal of the area around the core comes from the pulp around it, it was partially cut off such that the shown shape is not perfectly circular.

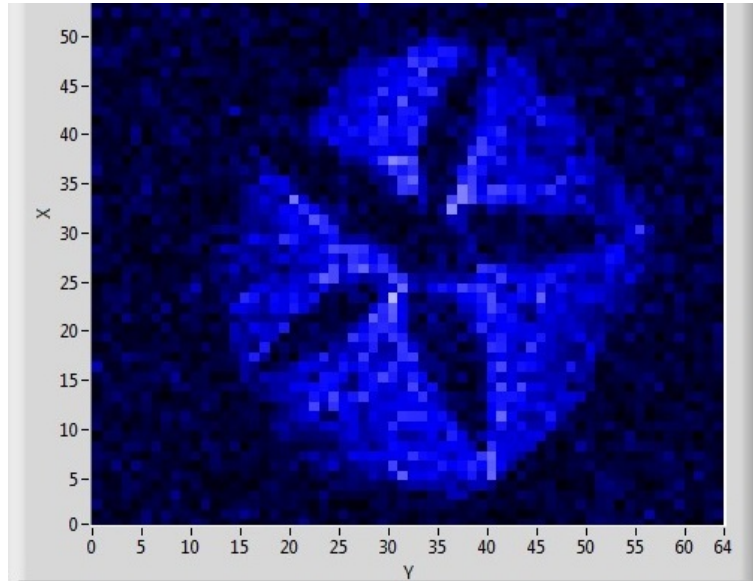


**Figure 16:** *Sample of an apple core sliced horizontally*

#### IV. DISCUSSION - THIMO PREIS

The setup in the first two parts of the experiment was not isolated very well thermally such that the  $B_0$  magnetic field was very sensitive to work with. The skew available for varying  $B_0$  is furthermore very unprecise and does not increase or decrease  $B_0$  consistently with a consistent rotating motion. It was therefore very difficult to calibrate the working frequency, which again is only necessary due to the ineffective thermal shielding with styrofoam, consistently after every measurement due to the unprecise adjustability of  $B_0$ . One should therefore improve the thermal shielding of the Minispec p20 magnet in order to render the ongoing calibration of the working frequency after every measurement unnecessary in the boundaries of the setups precision. One should furthermore increase the number of possible data points for the used fit of  $T_1$  and  $T_2$  in order to increase the precision of the measured values. This can easily be achieved by expanding the available LabView program to guarantee more than ten data points to be accounted for in the fit. One could furthermore refine the step size of the switches of the Minispec p20 electronic unit in order to account for more data points in the steeply falling/rising range of the exponential decay/rise. In total it would improve the precision of the measured results a lot if one would simply increase the number of taken data points during the measurement and also increase the number of measurements and



thus improve on the fits in order to average out the huge systematic errors due to the sensitivity of the apparatus on the chosen peak window and on the thermal shielding. One should furthermore be provided with theoretical values of the relaxation times in order to guarantee a successful discussion of the measured values and a prompt error evaluation during the experiment for measured values way off the theoretical values. These error sources had a higher impact on the first part of the measurement than on the second part concerned with the chemical shift. The systematic errors averaged out due to the structure of the measurement relying only on differences between the peaks.

The third part of the experiment went very smooth as the Bruker NMR analyzer mq7.5 was thermally shielded very well (compare 3.2) and had a high image resolution, only the intrinsic magnetic field inhomogeneities distorted our images a bit. By trying out the different slicing methods we could nevertheless achieve images of high resolution from which we could draw important physical conclusions.

The instruction manual [1] gives a clear introduction to the NMR concepts. The third part concerned with "Imaging with NMR" is too in depth for this experiment and misses to convey the quintessential points of this method. One should therefore cut down the explanation of the actual Fourier transformation of the NMR signal and in contrast should go more in depth in explaining the actual two dimensional data acquisition and on how the Helmholtz coils were set up in order to guarantee linear gradient fields.

Alltogether this experiment is very instructive in conveying the important NMR methods used throughout the medical and food sector in an engaging way. Only the first part of the experiment could be improved in order to increase the precision of the measured results as discussed above.

## REFERENCES

- [1] F61 - Nuclear Magnetic Resonance in the Advanced Students Laboratory. Url:  
<https://www.physi.uni-heidelberg.de/Einrichtungen/FP/anleitungen/F61.pdf>
- [2] The Basics of NMR by Joseph P. Hornak URL:  
<http://www.cis.rit.edu/htbooks/nmr>
- [3] Spin-lattice relaxation. Url:  
[https://en.wikipedia.org/wiki/Spin-lattice\\_relaxation](https://en.wikipedia.org/wiki/Spin-lattice_relaxation)
- [4] Gadolinium Wikipedia article, Url:  
<https://en.wikipedia.org/wiki/Gadolinium>
- [5] Indirect dipole-dipole coupling, Url:  
<https://en.wikipedia.org/wiki/J-coupling>
- [6] Spin echo method, Url:  
[https://en.wikipedia.org/wiki/Spin\\_echo](https://en.wikipedia.org/wiki/Spin_echo)

- [7] Fluorine atom information, Url:  
<https://en.wikipedia.org/wiki/Fluorine>